Prescribing stratospheric chemistry overestimates southern hemisphere climate change during austral spring in response to quadrupled CO_2

Feng Li[1,2,3] · Paul A. Newman[2]

Abstract

The interaction of stratospheric chemistry with a changing climate from an abrupt CO_2 quadrupling is assessed using the coupled atmosphere–ocean Goddard Earth Observing System Chemistry-Climate Model (GEOSCCM). Two abrupt $4 \times CO_2$ experiments were performed, one with interactive stratospheric chemistry and the other with a prescribed stratospheric chemistry that does not simulate stratospheric ozone response to $4 \times CO_2$. The interactive and prescribed chemistry experiments simulate similar global mean surface temperature change. Nevertheless, interactive chemistry is critical to capture the Southern Hemisphere tropospheric midlatitude jet response to $4 \times CO_2$. When stratospheric ozone response to $4 \times CO_2$ is neglected, GEOSCCM overestimates Southern Hemisphere tropospheric circulation change. This stratospheric chemistry-induced climate impact has large seasonal variability. During the austral spring season September–October–November (SON), prescribed chemistry yields a stronger poleward shift and intensification of the Southern Hemisphere midlatitude tropospheric jet, surface wind stress, and the Southern Ocean meridional overturning circulation than occurs with interactive chemistry. In other seasons interactive and prescribed chemistry have similar effects on the Southern Hemisphere circulation. The seasonality of stratospheric chemistry-induced climate impact is related to the seasonality of Antarctic lower stratospheric ozone response to $4 \times CO_2$. In contrast to this stratospheric ozone response to $4 \times CO_2$, stratospheric ozone recovery from decline of the ozone depleting substances has its largest impact on the Southern Hemisphere tropospheric circulation in austral summer (December–January–February), but no effects in SON. It is found that the different seasonality for these two stratospheric ozone layer change scenarios is related to the different seasonality of tropopause meridional temperature gradient response.

Keywords Stratospheric ozone feedback · Interactive and prescribed stratospheric chemistry · Stratosphere-troposphere coupling · Southern hemisphere midlatitude jet · Stratospheric ozone recovery

1 Introduction

The stratospheric ozone layer is strongly affected by increases of atmospheric carbon dioxide (CO_2). Increased CO_2 cools the stratosphere and strengthens the Brewer-Dobson circulation (Butchart et al. 2006, 2010). This leads

to an ozone increase in the upper stratosphere and an ozone decrease in the tropical lower stratosphere (Shepherd 2008; Li et al. 2009). Because ozone is also a greenhouse gas, the stratospheric ozone response to increased CO_2 affects surface temperature. This stratospheric ozone feedback also modifies the stratospheric water vapor feedback process, because ozone-induced tropical lower stratospheric cooling reduces stratospheric water vapor increase in a warming climate (Dietmüller et al. 2014; Nowack et al. 2015; Marsh et al. 2016). The combined effects of the stratospheric ozone feedback and the accompanying reduced stratospheric water vapor feedback is the total stratospheric chemical feedback (Nowack et al. 2015).

The magnitude of the stratospheric chemical feedback, which is quantified by comparing global-mean surface

✉ Feng Li
feng.li@nasa.gov

1 Universities Space Research Association, Columbia, MD, USA

2 NASA Goddard Space Flight Center, Greenbelt, MD, USA

3 Present Address: University of Maryland, Baltimore County, Baltimore, USA

temperature changes in abrupt $4 \times CO_2$ experiments with and without interactive stratospheric ozone chemistry, is strongly model dependent. Nowack et al. (2015) found that the stratospheric chemical feedback causes a 20% reduction of surface warming in the Hadley Centre Global Environmental Model version 3, but other modeling groups showed much weaker or even negligible effects on the global-mean surface temperature (Dietmüller et al. 2014; Marsh et al. 2016; Chiodo and Polvani, 2019). The cause of this large spread of modeled stratospheric chemical feedback is an ongoing research topic.

The stratospheric ozone response to $4 \times CO_2$ also affects tropospheric circulation through stratosphere-troposphere dynamical coupling (Chiodo and Polvani, 2017; 2019). This effect is not directly related to the strength of the stratospheric chemical feedback on surface temperature. Chiodo and Polvani (2017) showed that even though the stratospheric chemical feedback on global-mean surface temperature is negligible in the NCAR Community Earth System Model (CESM), neglecting the stratospheric ozone interaction results in significant overestimation of the poleward shift of the Southern Hemisphere (SH) tropospheric midlatitude jet in response to $4 \times CO_2$. Chiodo and Polvani (2019) also found that stratospheric ozone response to $4 \times CO_2$ mitigates North Atlantic climate during the Northern Hemisphere (NH) winter. These studies demonstrate the importance of including interactive stratospheric chemistry for assessing future climate change.

The stratospheric ozone response to $4 \times CO_2$ has large seasonal variations mainly due to the seasonal variability of stratospheric transport, particularly in polar regions (e.g., Chiodo et al. 2018). Because of the seasonal variations of stratospheric ozone, with contributions from the seasonal variation of insolation, the stratospheric ozone induced tropospheric climate impact also has large seasonal variations. Chiodo and Polvani (2019) found that the largest interactive ozone impact on SH tropospheric circulation is in December–January–February (DJF). Interestingly, the projected stratospheric ozone recovery, due to the decline of the ozone depleting substances (ODSs), also has the largest effects on SH tropospheric circulation in DJF. While the seasonality of ODS-induced stratospheric ozone recovery and its climate impact is extensively studied, the seasonal variations of stratospheric ozone response to $4 \times CO_2$ and its associated climate effects are not well understood.

This study's main purpose is to understand the seasonal variability of stratospheric ozone responses to $4 \times CO_2$ and its impact on tropospheric and ocean circulations using the coupled atmosphere–ocean Goddard Earth Observing System—Chemistry Climate Model (GEOSCCM). When stratospheric ozone chemistry is not included, GEOSCCM significantly overestimates the SH tropospheric and Southern Ocean circulation response to $4 \times CO_2$ during the austral

spring season September–October–November (SON). However, neglecting stratospheric ozone chemistry doesn't significantly affect SH climate change during DJF. Thus, another purpose of this study is to understand differences between ODS-induced stratospheric ozone recovery and CO_2-induced stratospheric ozone changes, particularly their seasonality of tropospheric impact.

2 Model and experiments

The main components of the coupled atmosphere–ocean GEOSCCM are the GEOS atmospheric general circulation model (Molod et al. 2012), the Geophysical Fluid Dynamics Laboratory Modular Ocean Model version 5 (Griffies 2012), the Los Alamos Sea Ice Model (Hunke and Lipscomb 2008), and a comprehensive stratospheric chemistry model (Pawson et al. 2008; Oman and Douglass 2014). The atmospheric model has 72 levels to the top at 0.01 hPa. The ocean model has 50 layers with fine resolution of 10 m in the top 200 m. More details of the coupled atmosphere–ocean GEOSCCM were described in Li et al. (2016) and Li and Newman (2020). The simulations used in this study are conducted with horizonal resolution of $1°$ longitude $\times 1°$ latitude for both the atmosphere and ocean models.

GEOSCCM's comprehensive stratospheric chemistry model includes all the important stratospheric gas phase and heterogeneous reactions (Pawson et al. 2008). The stratospheric chemistry is coupled with model radiation and physics. Radiatively important stratospheric trace species, including O_3, H_2O, CH_4, N_2O, CFC-11, CFC-12, and HCFC-22, are calculated from the chemistry model and used in the radiation code. In addition to the full stratospheric chemistry model, we can also prescribe the stratospheric chemistry in GEOSCCM. This simple prescription is for monthly and zonally mean O_3, CH_4, N_2O, CFC-11, CFC-12, and HCFC-22. These fields are derived from an atmosphere only GEOSCCM interactive stratospheric chemistry simulation. They are set as the middle-month values and linearly interpolated to each time step. Stratospheric water vapor in the prescribed chemistry is controlled by physical processes.

We have performed two abrupt $4 \times CO_2$ experiments with interactive stratospheric chemistry (IC simulation) and prescribed stratospheric chemistry (PC simulation). Both experiments start after a 200 year spin-up with perpetual year 2000 forcings. Each experiment includes a 50 year baseline simulation with fixed year 2000 forcings, followed by a 150 year simulation where CO_2 is quadrupled. We define the climate response to $4 \times CO_2$ as the differences between the last 100 years of the $4 \times CO_2$ simulation and the 50 year baseline simulation. Climate response in IC includes the effects of the stratospheric chemical feedback. However, in the PC experiment, ozone, CH_4, N_2O, CFC-11, CFC-12,

and HFCF-22, in both the baseline and the $4\times CO_2$ simulations are relaxed to their prescribed year 2000 fields (the prescribed O_3 field is shown in Fig. S1a). Thus, climate response in PC does not include the effects of changes of both stratospheric ozone and other radiatively important species. The climate impact of interactive stratospheric chemistry is quantified as the different responses to $4\times CO_2$ between IC and PC. Note that our experiments are based on year 2000 conditions with high ODS loading, which is a major difference from previous studies that were based on the preindustrial conditions (Nowack et al. 2015; Marsh et al. 2016; Chiodo and Polvani 2019).

We have also analyzed two additional simulations of the twenty-first century (2005–2099) to investigate the differences between ODS-induced stratospheric ozone recovery and $4\times CO_2$-induced stratospheric ozone changes, including their climate impact. Each simulation ensemble has four members that differ in initial conditions. Both ensembles use interactive stratospheric chemistry. The Control ensemble is forced with the Representative Concentration Pathway 6.0 greenhouse gas (GHG) scenario and the WMO-2014 baseline (A1) ODS scenario. The HighODS ensemble has the same setup as the Control ensemble except that the ODSs are fixed at year 2005 levels. The HighODS ensemble does not simulate ODS-induced stratospheric ozone recovery at the end of the twenty-first century. The climate impact of ODS-induced stratospheric ozone recovery is defined as the ensemble-mean differences between the HighODS and Control (HighODS minus Control) of the last 20 years of the simulations. We note that the HighODS has stratospheric ozone levels at year 2005, not at year 2000 as in the PC $4\times CO_2$ experiment. This difference is small, and does not affect the comparison between ODS-induced stratospheric ozone recovery and $4\times CO_2$-induced stratospheric ozone changes.

3 Results

3.1 Annual-mean results

The ozone layer is significantly changed by a CO_2 quadrupling ($4\times CO_2$), as has been shown in other chemistry-climate models [Nowack et al. 2015; Marsh et al. 2016; Chiodo et al. 2018]. These changes are a near latitudinal-uniform increase in the middle and upper stratosphere, a decrease in the tropical lower stratosphere, and an increase in the extratropical lower stratosphere. Stratospheric ozone changes in our IC experiment are consistent with these previous studies. Upper stratospheric ozone increases by more than 30% and the tropical lower stratospheric ozone decreases by up to 30% (Fig. 1a). Increasing CO_2 cools the stratosphere with a maximum at the stratopause (Fig. 1b).

This cooling slows gas-phase photochemical ozone loss reactions, leading to ozone increases (Jonsson et al. 2004). Unlike the photochemistry-controlled upper stratospheric ozone, the lower stratospheric ozone is strongly affected by transport (Shepherd 2008). A robust feature of stratospheric dynamical response to increased CO_2 is an acceleration of the Brewer-Dobson circulation with enhanced tropical upwelling and extratropical downwelling (Butchart et al. 2006, 2010; Li et al. 2008). The enhanced tropical upwelling causes an ozone decrease in the tropical lower stratosphere by advecting ozone-poor tropospheric air more quickly upward. Enhanced extratropical downwelling increases downward advection of ozone-rich upper stratospheric air into the extratropical lower stratosphere. The stronger NH ozone downwelling advection (due to increased CO_2) creates a clear hemispheric asymmetry in the lower stratosphere (Li et al. 2009). Extratropical ozone decreases around the tropopause. As the tropopause height rises with $4\times CO_2$, the layer that is just above the tropopause in the baseline simulation shifts to troposphere, and air in that layer changes from stratospheric ozone-rich air to tropospheric ozone-poor air, leading to ozone decrease in the extratropical tropopause region (Dietmüller et al. 2014).

Stratospheric water vapor is increased by the quadrupled CO_2 (Fig. 1c). This increase is caused by higher temperatures at the tropical tropopause region that allows higher concentrations of tropospheric water to be transported into the stratospheric overworld (Dessler et al. 2013; Banerjee et al. 2019; Li et al. 2020). The pattern and magnitude of stratospheric water vapor changes in the IC experiment (Fig. 1c) are within the large range reported by the Coupled Model Intercomparison Project (CMIP5) models (Banerjee et al. 2019).

The zonal wind field is also changed by quadrupled CO_2 (Fig. 1d). The subtropical upper tropospheric jets in both hemispheres are accelerated, with maximum accelerations on the upper equatorial flanks. The SH tropospheric extratropical jet shifts poleward with westerly anomalies over 50–70°S and easterly anomalies over 30–50°S. In the stratosphere, the extratropical westerly jet and lower stratosphere subtropical jet strengthens. These results are consistent with previous studies of CO_2-induced zonal mean circulation changes (e.g., Kushner et al. 2001; Lu et al. 2008).

The IC climate changes (Fig. 1) include stratospheric chemical feedback effects. These effects are quantified by the different responses to $4\times CO_2$ between the PC and IC experiments (PC minus IC). PC does not simulate stratospheric ozone response to $4\times CO_2$—it fails to capture ozone increase in the upper stratosphere and polar lower stratosphere and ozone decrease in the tropical lower stratosphere (Fig. 2a). These PC stratospheric ozone differences cause cooling in the upper stratosphere and extratropical lower stratosphere and warming in the tropical lower stratosphere
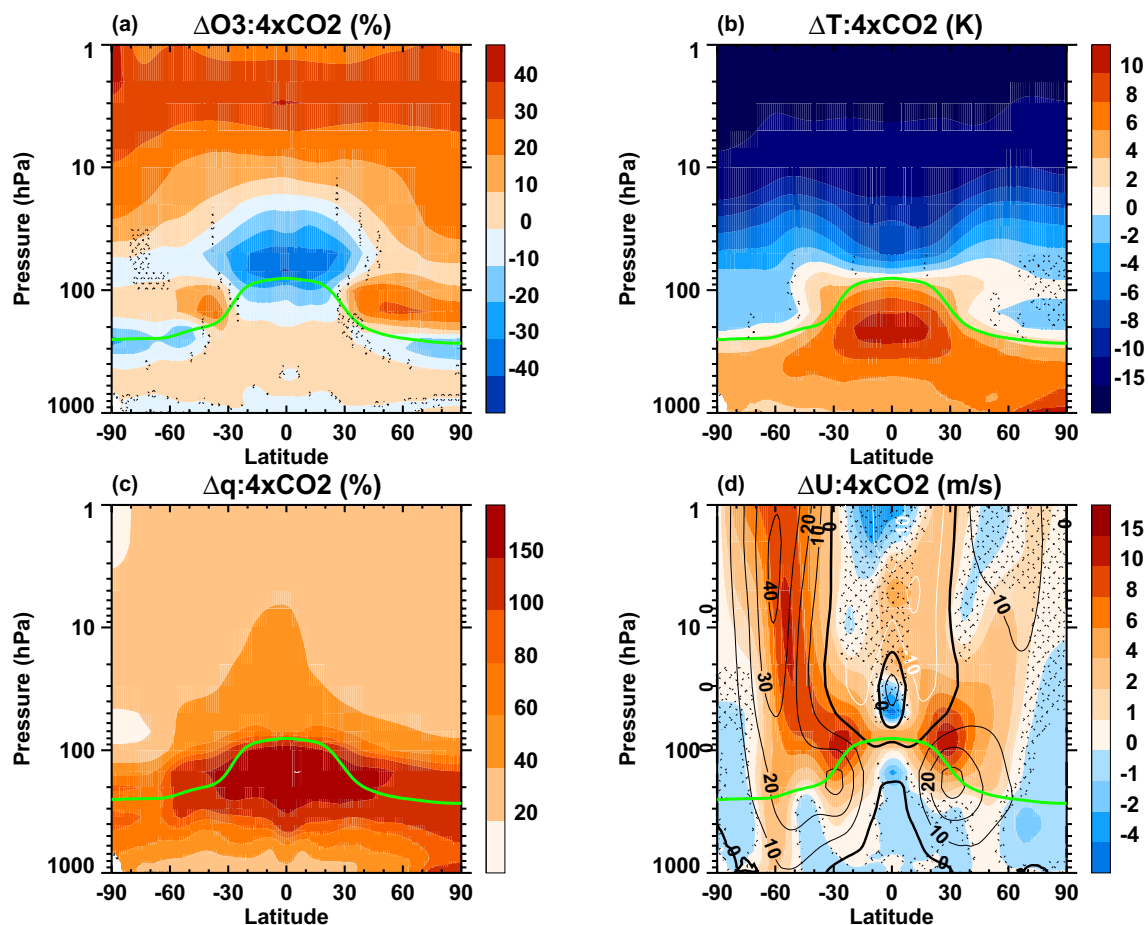
Fig. 1 Responses to 4×CO₂ with respect to the baseline in the IC experiment: annual and zonal mean (**a**) ozone, (**b**) temperature, (**c**) water vapor, and (**d**) zonal wind. Unit for ozone and water vapor is percentage relative to the baseline values. Contours in (**d**) are zonal wind climatology in the baseline. Green line is the climatological tropopause level in the 4×CO₂ simulation. Stippling indicates that the response is not statistically significant at the two-tailed 5% level

(Fig. 2b), mainly due to changes in ozone shortwave radiation absorption. The warmer tropical lower stratosphere leads to stronger stratospheric water vapor increase. The stratospheric water vapor response to 4×CO₂ in PC is about 30% larger than that in IC (Fig. 2c).

Because stratospheric ozone and water vapor are greenhouse gases, the different responses of stratospheric ozone and water vapor in the IC and PC 4×CO₂ simulations influence surface warming in these two experiments. The strength of the stratospheric chemical feedback is quantified by the difference in the climate feedback parameter between IC and PC. We use the Gregory linear regression method (Gregory et al. 2004) to calculate the climate feedback parameter. Here we follow Andrew et al. (2015) by linearly fitting years 21–150 of the 4×CO₂ simulations. Table 1 shows that climate feedback parameters in the IC and PC experiments are − 0.85 and − 0.83 W m⁻² K⁻¹, respectively. Thus, the stratospheric chemical feedback parameter from GEOSCCM is − 0.02 W m⁻² K⁻¹, which reduces the

equilibrium global-mean surface temperature response to 4×CO₂ by 0.16 K, or about 2.4%. This GEOSCCM stratospheric chemical feedback is at the lower end of the previous reported values and agree with some of the previous studies (Marsh et al. 2016; Chiodo and Polvani 2019).

In the lower stratosphere, PC causes warming in the tropics and cooling in the extratropics relative to IC (Fig. 2b), which is mainly driven by changes in ozone shortwave absorption (not shown). This PC meridional pattern exceeds the lower stratospheric negative equator-to-pole temperature gradient in IC (Fig. 1b). PC simulates a stronger stratospheric midlatitude westerly response (Fig. 2d), consistent with the stronger lower stratospheric temperature gradients via the thermal wind relationship. In the SH, the overly strong midlatitude westerly response extends from the stratosphere into the troposphere, significantly enhancing the tropospheric midlatitude jet response to 4×CO₂. Changes in the NH midlatitude jet are not significantly different between IC and PC, partly because the NH midlatitude jet is not zonally
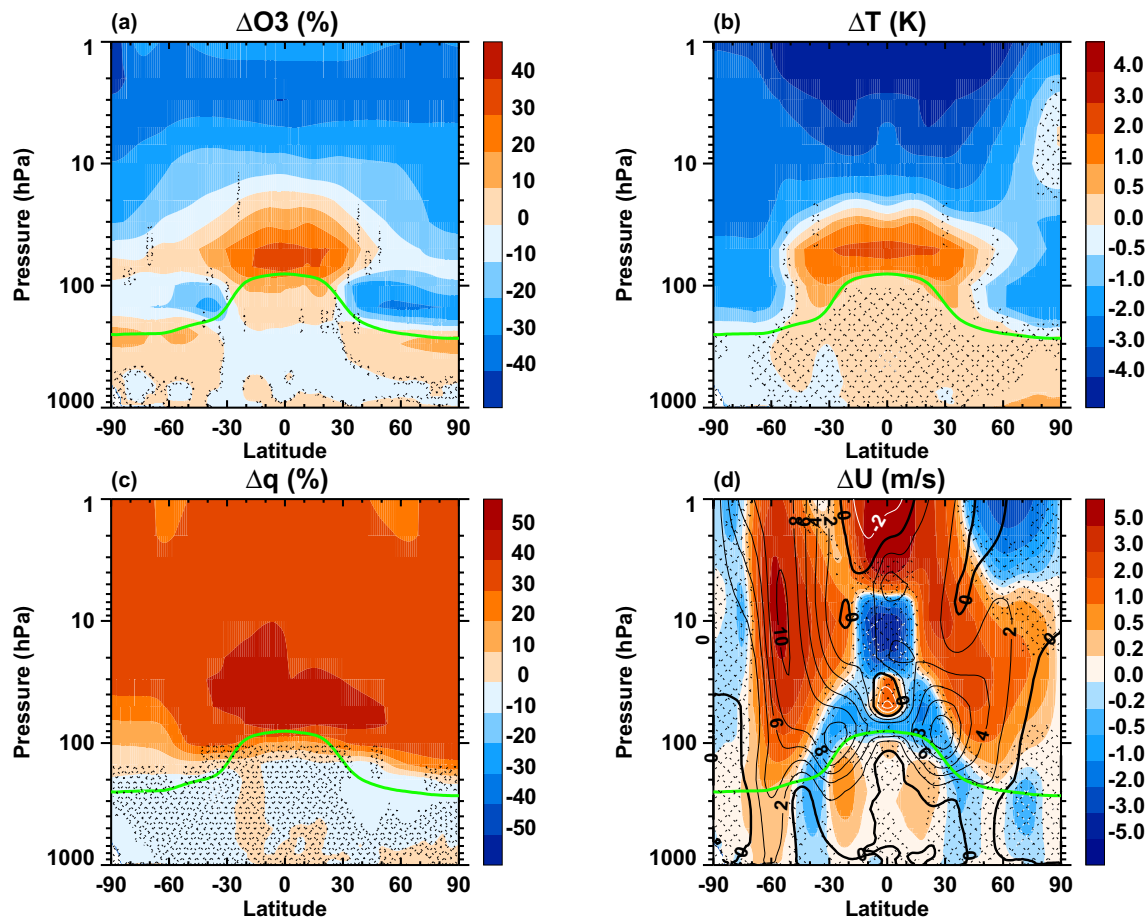
Fig. 2 Different response to $4\times CO_2$ between the PC and IC experiment (PC minus IC): annual and zonal mean (**a**) ozone, (**b**) temperature, (**c**) water vapor, and (**d**) zonal wind. Unit for ozone and water vapor is percentage relative to the IC baseline values. Contours in (**d**) are the IC zonal wind changes in response to $4\times CO_2$. Green line is the climatological tropopause level in the IC experiment. Stippling indicates that the difference is not statistically significant at the two-tailed 5% level

Table 1 The climate feedback parameter (α) and the equilibrium surface air temperature response to $4\times CO_2$ (ΔT_e) in the interactive and prescribed chemistry experiments

Experiment	α (W m^{-2} K^{-1})	ΔT_e (K)
Interactive chemistry	-0.85	6.51
Prescribed chemistry	-0.83	6.67

Table 2 Annual-mean and seasonal changes in the Southern Hemisphere tropospheric midlatitude jet location and strength in response to $4\times CO_2$

	Interactive Chemistry		Prescribed Chemistry	
	Location (°)	Strength (m/s)	Location (°)	Strength (m/s)
Annual	-2.9	**1.5**	-3.0	**1.6**
SON	**-0.6**	**1.3**	**-2.1**	**2.1**
DJF	-3.5	1.0	-3.4	0.9
MAM	**-2.9**	1.7	**-2.5**	1.6
JJA	-1.0	1.8	-2.0	2.0

The tropospheric midlatitude jet location and strength is defined as the latitude and magnitude of the 850 hPa zonal-mean zonal wind maximum, respectively. Negative number in location change indicates southward shift. The bold numbers in the shaded cells mean that the results are statistical significantly different between the interactive and prescribed chemistry experiments

symmetric and zonal averaging smears out the stratospheric chemistry impact. For example, Fig. S2 shows that neglecting stratospheric chemistry leads to opposite changes of the 850 hPa jet over the North Atlantic and North Pacific. The PC experiment also overestimates the acceleration of the subtropical upper tropospheric jet, which is more pronounced in the SH.

The $4\times CO_2$ IC simulation shifts the annual-mean SH midlatitude lower troposphere (850 hPa) jet maximum poleward by 2.9 degrees and strengthens it by 1.5 m/s with respect to its baseline (Table 2). The PC simulation significantly overestimates SH midlatitude jet strengthening, amplifying the jet maximum by 0.2 m/s (12%). PC also

amplifies the poleward shift of the SH 850-hPa jet by 0.1 degree, although the change is not statistically significant. Our results are consistent with Chiodo and Polvani (2017), who first reported reduction in the SH tropospheric jet response to $4 \times CO_2$ due to interactive stratospheric ozone chemistry.

3.2 Seasonal variations

Because of the strong seasonality of stratospheric transport, the IC stratospheric ozone layer response to $4 \times CO_2$ has large seasonal variability, particularly in the Antarctic lower stratosphere. The IC experiment simulates descent of the upper stratospheric ozone-rich air into the polar regions from the Brewer-Dobson circulation's deep branch with strongest downwelling in winter (Fig. 3). During the SH spring (SON),

high-ozone air descends to the Antarctic lower stratosphere, with more than 40% increase at 150–50 hPa (Fig. 3a). However, ozone decreases around 60°S in 70–30 hPa. During the SH summer (DJF), Antarctic ozone deceases at 100–50 hPa (Fig. 3b). In the Arctic lower stratosphere ozone increases in all seasons, with smaller seasonal variations than its SH counterpart.

What causes Antarctic ozone decrease in austral spring and summer? Mixing of low latitude ozone-depleted air may play a role in summer, but not in spring when the Antarctic polar vortex barrier is still strong. Figures 4a–c show the IC monthly ozone response to quadrupled CO_2 from October to December. In October the Antarctic negative ozone anomalies are located in the middle stratosphere, above and equatorward of the large positive ozone anomalies. In November and December, the negative ozone anomalies
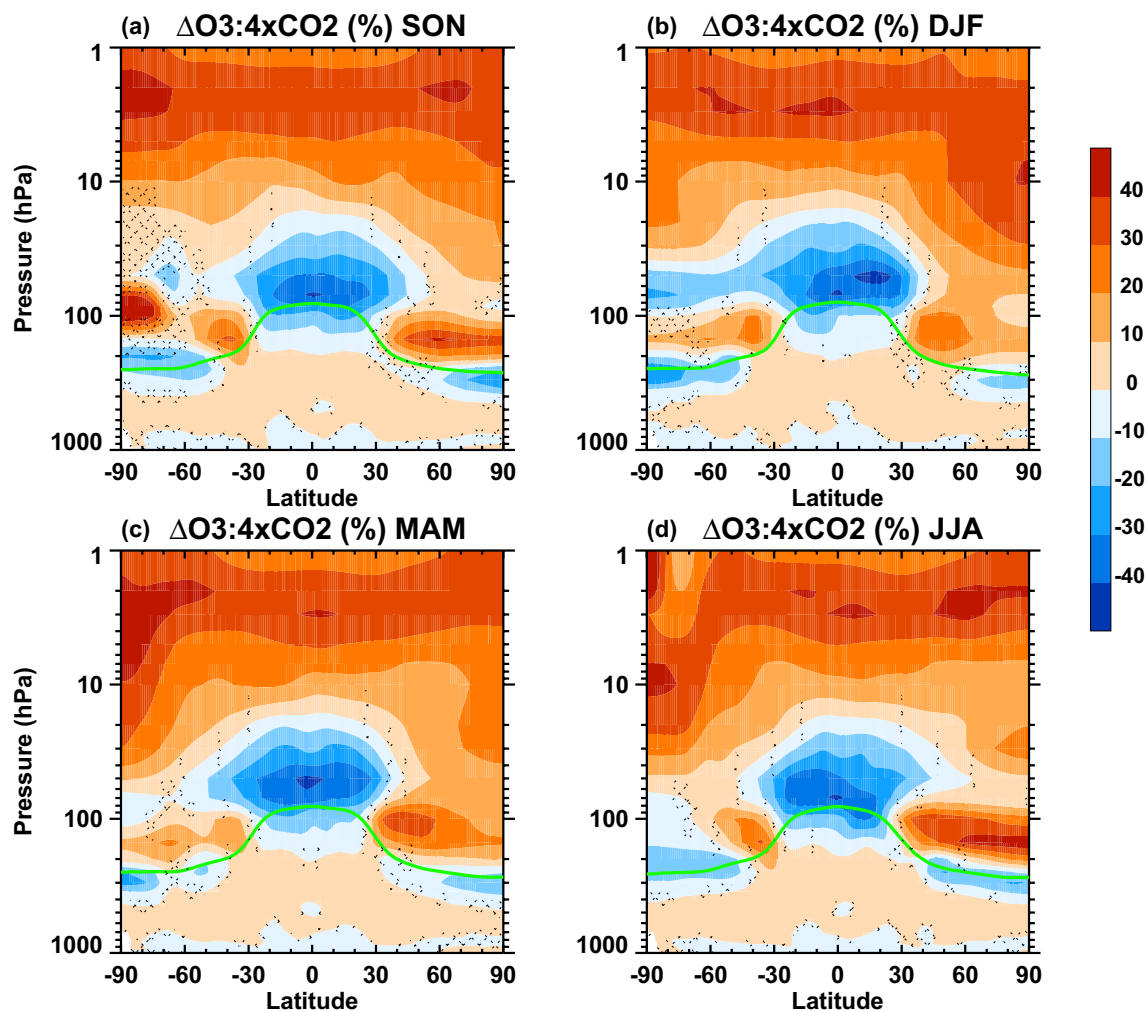

Fig. 3 The IC ozone responses to $4 \times CO_2$ with respect to its baseline in **a** September–October–November (SON); **b** December–January–February (DJF); **c** March–April–May (MAM); and **d** June–July–August (JJA). Unit is percentage relative to the IC baseline values. Green line is the seasonal mean tropopause level. Stippling indicates that the response is not statistically significant at the two-tailed 5% level
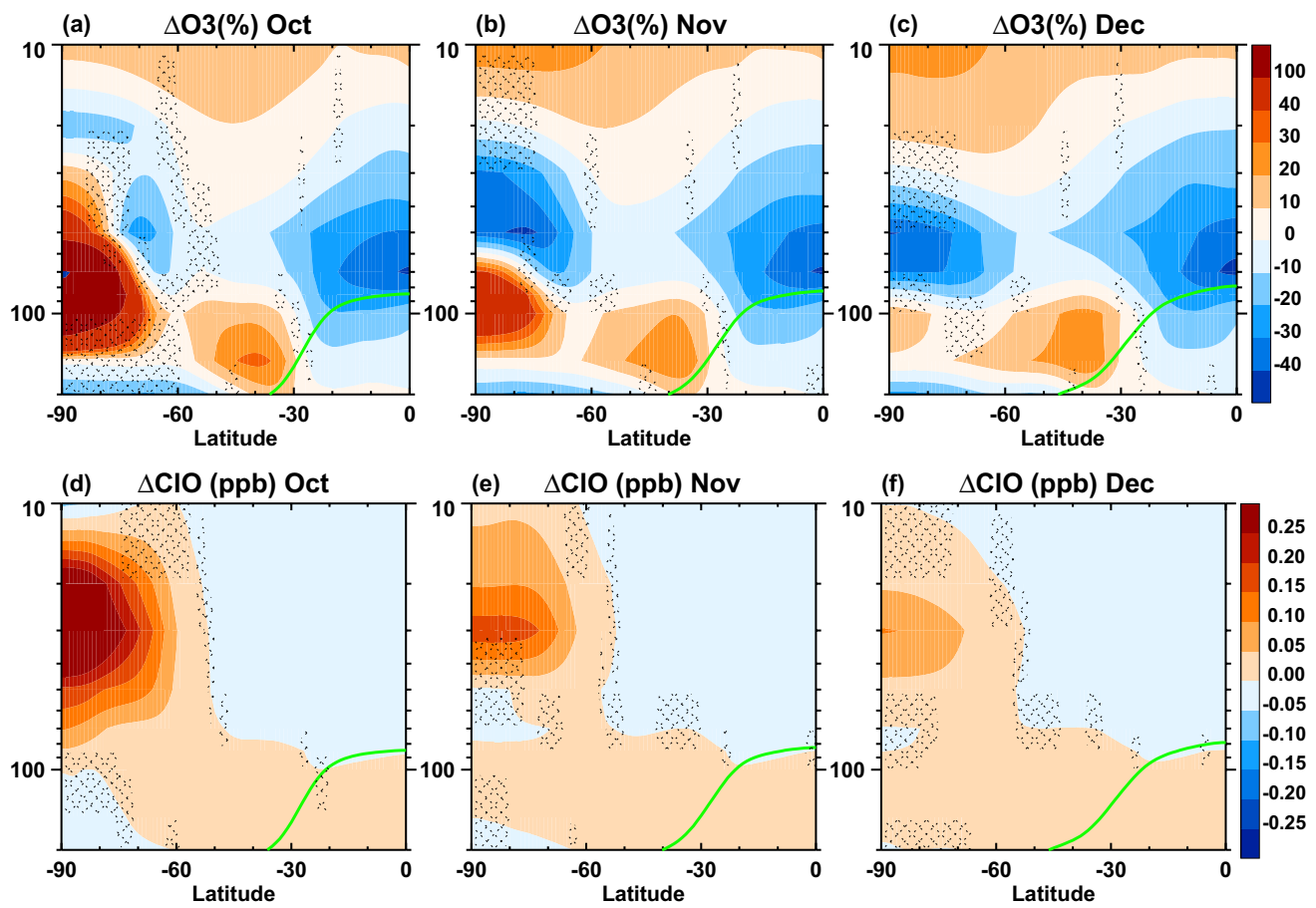
Fig. 4 **a–c** The IC ozone responses to $4 \times CO_2$ with respect to its baseline in October, November, and December; **d–f** Same as **a–c**, but for Chlorine Monoxide (ClO) response. Stippling indicates that the response is not statistically significant at the two-tailed 5% level

become stronger and descend to the lower stratosphere. The transport of low latitude ozone-poor air into the Antarctica is suppressed by the vortex barrier even in December. Thus, the summer Antarctic lower stratospheric negative ozone anomalies originate from the spring middle stratosphere. Remember that our experiment is based on year 2000 conditions with high ODS loading. A possible explanation for Antarctic springtime ozone decrease is enhanced heterogeneous ozone destruction reactions. Increased CO_2 causes Antarctic stratosphere cooling (Fig. 1b), which can enhance the formation of polar stratospheric clouds, leading to stronger heterogenous chlorine activation and catalytic ozone loss reactions. Indeed, the IC experiment simulates significant increase of ClO, a crucial reactive chlorine species, in the Antarctic lower stratosphere centered at 30 hPa from October to December (Fig. 4d–f). Therefore, heterogeneous chemistry is also important in determining the Antarctic lower stratospheric ozone response to quadrupled CO_2 in our experiment.

The PC experiment does not capture these seasonal ozone responses to quadrupled CO_2. Hence, PC ozone in the Antarctic lower stratosphere is too low during SON and too high during DJF with respect to the IC ozone. Associated with its large Antarctic lower stratospheric ozone decrease relative to IC, the strongest PC cooling relative to IC occurs in SON (Fig. 5a). However, in DJF PC has a warmer Antarctic lower stratosphere than IC between ~ 100 and 40 hPa (Fig. 5b), coincident with its higher ozone. The relationship between the seasonal evolution of Antarctic lower stratospheric temperature and ozone anomalies (PC minus IC) can be more clearly seen in Fig. 6. A prominent feature of Fig. 6 is the coherent descending of cold/warm temperature (Fig. 6a), low/high ozone (Fig. 6b), and shortwave cooling/warming (Fig. 6d) in the mid-to-lower stratosphere from September to February. As discussed in Fig. 4, the PC ozone increase is mainly because the IC ozone is destroyed by enhanced heterogenous reactions in austral spring. Figure 6 indicate that while dynamical ozone response leads to PC spring Antarctic lower stratospheric cooling, chemical ozone response is a major driver of PC summer Antarctic lower stratospheric warming in our experiment.
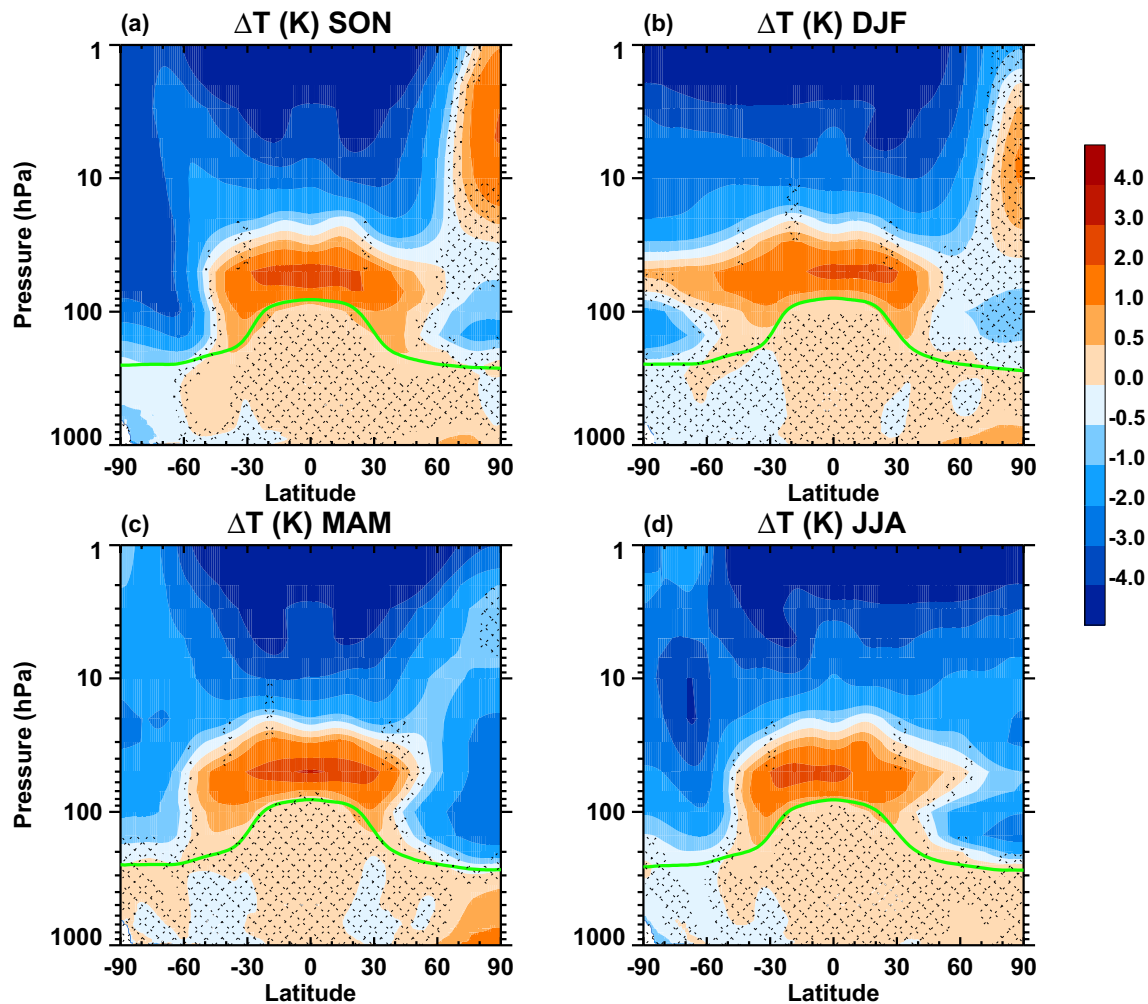
Fig. 5 Different response in the zonal-mean temperature to $4 \times CO_2$ between the PC and IC experiment (PC minus IC) in (**a**) September–October–November (SON); **b** December–January–February (DJF); **c** March–April–May (MAM); and **d** June–July–August (JJA). Green line is the seasonal mean tropopause level in the IC experiment. Stippling indicates that the difference is not statistically significant at the two-tailed 5% level

The modification of stratospheric water vapor response to $4 \times CO_2$ by ozone interaction, and the responses of CH_4, N_2O, CFC-11, CFC-22, and HCFC-22 to $4 \times CO_2$ also have seasonal variations. The different seasonal responses of these species in the PC with respect to IC affect longwave radiation. However, longwave radiation is mainly dependent on temperature. PC has longwave warming during SON and longwave cooling during DJF relative to IC in the Antarctic lower stratosphere (not shown), consistent with PC's lower temperature in SON and higher temperature in DJF. Therefore, the seasonality of lower stratospheric temperature is strongly driven by the seasonality of the stratospheric ozone response to $4 \times CO_2$ and the associated ozone shortwave absorption.

Stratospheric ozone, radiation, and dynamics are strongly coupled. Thus, changes in stratospheric ozone and radiation

also modify the stratospheric dynamics response to $4 \times CO_2$, which affects stratospheric temperature. Figure 6c shows that the PC simulation induces dynamical cooling in SON and dynamical heating in DJF, which contribute to lower stratospheric cooling in SON and warming in DJF. Indeed, in SON cooling near the tropopause (about 200 hPa) in PC is mainly driven by dynamics. According to the linear theory, the favorable background zonal wind condition for upward Rossby wave propagation is weak westerlies. The PC vortex is stronger than the IC vortex associated with a stronger PC meridional temperature gradient. This stronger PC jet prohibits upward Rossby wave propagation in SON when the vortex is strong, but favors vertical propagation of Rossby wave in DJF when the vortex breakdown is delayed (Lin et al. 2017). These Rossby wave vertical propagation
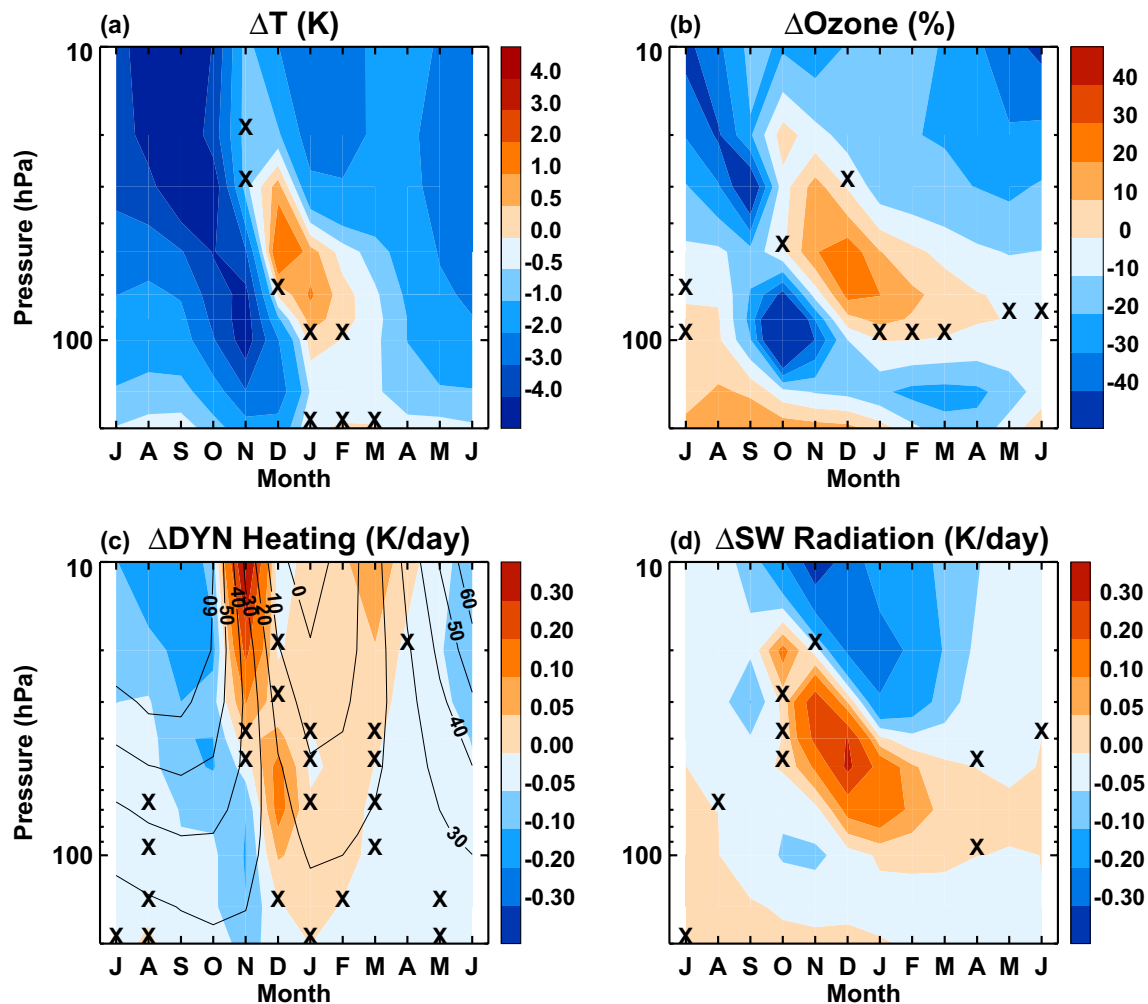
Fig. 6 Seasonal evolution of the different response to $4 \times CO_2$ between the PC and IC experiment (PC minus IC) in Antarctic (averaged over 65–90°S) (**a**) temperature, (**b**) ozone, (**c**) dynamical heating rate, and (**d**) shortwave hearting rate. Contours in (**c**) are climatological circumpolar zonal wind (averaged over 50–70°S) in the IC experiment. Cross indicates that the difference is not statistically significant at the two-tailed 5% level

and dissipation changes contribute to PC Antarctic lower stratospheric springtime cooling and summertime warming.

Neglecting the strong coupling between stratospheric ozone and Antarctic polar vortex strongly underestimates Antarctic polar vortex interannual variability. IC simulates large Antarctic polar vortex interannual variability in austral spring and early summer with strong variations in the polar temperature and circumpolar jet strength as measured by the zonal-mean zonal wind at 60°S (see contours in Fig. 7). PC only produces about half of the variability in Antarctic lower stratospheric temperature at 200–20 hPa in October-January (Fig. 7a). PC also significantly reduces the variability of circumpolar jet strength (Fig. 7b). The largest decrease occurs in November and December around 10 hPa, indicating that the PC experiment does not capture the variability of the timing of vortex breakdown into summer conditions. The

standard deviation of the Antarctic polar vortex breakdown date, defined as when the zonal mean zonal wind at 60°S and 10 hPa changes from westerly to easterly, is 20% smaller in PC (8.3 days) than in IC (10.3 days).

We have shown in Sect. 3.1 that PC simulates stronger annual-mean SH midlatitude jet response to $4 \times CO_2$ (see Fig. 2d). Comparing Fig. 8 with Fig. 2d reveals that the PC's stronger annual-mean SH tropospheric zonal wind response is dominated by that in SON. PC has larger stratospheric and tropospheric westerly changes at 50–70°S in SON relative to IC (Fig. 8a), consistent with the colder Antarctic lower stratosphere and the enhanced meridional temperature gradient (see Fig. 5a). Except in SON, PC does not significantly change the SH tropospheric midlatitude jet response to $4 \times CO_2$ in other seasons.
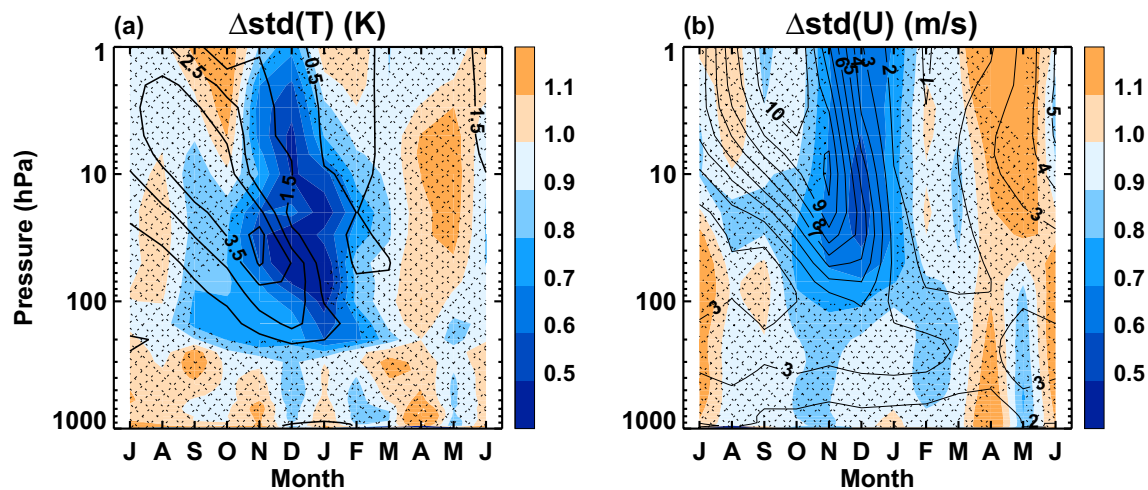
Fig. 7 a Contours are standard deviation of the Antarctic temperature (averaged over 65–90°S) in the last 100 years of the IC 4×CO$_2$ simulation. Color shading is the ratio between the PC and IC Antarctic temperature standard deviation (PC/IC). Stippling indicates that the standard deviations are not statistically significant different between PC and IC. **b** Same as (**a**), but for zonal-mean zonal wind at 60°S

Again, we use the 850 hPa zonal-mean zonal wind to quantify the seasonal impact of neglecting stratospheric chemistry on SH tropospheric circulation (Table 2). In SON, PC simulates a SH jet response to 4×CO$_2$ that shifts too much to the pole (1.5° or 250%) and is too strong (0.8 m/s or 62%) relative to the IC experiment. PC and IC have similar SH tropospheric jet response in other seasons, except in MAM when PC has weaker poleward shift.

The seasonality of stratospheric chemistry-induced tropospheric circulation impact in GEOSCCM is different from that in NCAR CESM. Chiodo and Polvani (2017, 2019) found that interactive ozone has the largest effects on SH tropospheric midlatitude jet in DJF, but no effects in SON (see Fig. S1 of Chiodo and Polvani, 2017). This difference is likely associated with different Antarctic lower stratospheric temperature changes between GEOSCCM and CESM, which are in turn related to different seasonal Antarctic lower stratospheric ozone and dynamics response to 4×CO$_2$. We note that the experimental setup is different between this study and Chiodo and Polvani (2017). Our abrupt 4×CO$_2$ experiments are based on the year 2000 conditions, which has much higher ODS loading than the 4×CO$_2$ simulations in Chiodo and Polvani (2017) that are based on the preindustrial conditions. The high ODS loading in our IC experiment leads to enhanced heterogenous ozone loss reactions in the springtime Antarctic middle/lower stratosphere in response to increased CO$_2$. As a result, PC has higher ozone, stronger shortwave radiation, and warmer temperature in the Antarctic lower stratosphere during DJF relative to IC. The warmer Antarctic lower stratosphere causes a smaller meridional temperature gradient increase, leading to weak stratospheric westerly changes. This can explain why interactive ozone

does not affect SH tropospheric circulation in DJF in our experiment.

3.3 Impact of stratospheric chemistry on southern hemisphere surface and southern ocean

The IC 4×CO$_2$ simulation drives a sea level pressure (SLP) decreases in the SH high latitudes and increases in the midlatitudes (Fig. 9a), indicating a shift toward the high index of the Southern annular mode in a warming climate. During SON the PC experiment amplifies these SLP changes with respect to IC (Fig. 9b). The magnitude of the excessive SLP changes is substantial: PC overestimates the IC SH high latitude SLP decrease (averaged over 60–90°S) by 1.5 hPa (a 150% increase) and the IC midlatitude SLP increase (averaged over 40–60°S) by 0.6 hPa (a 30% increase).

The strong surface westerlies over the Southern Ocean play a crucial role in ocean circulation and global climate. The location and strength of the SH midlatitude surface wind stress have profound effects on Southern Ocean surface Ekman transport, Meridional Overturning Circulation (MOC), and ocean water properties (e.g., Russell et al. 2006; Marshall and Speer 2012). In the IC response to 4×CO$_2$, westerly surface wind stress during SON increases in the 45–65°S band and decreases in the 30–45°S band (Fig. 10a). Associated with the poleward intensification of the surface wind stress, the wind stress curl decreases poleward of ~60°S and increase at ~40–60°S (Fig. 10c), indicating an increase of Ekman upwelling and pumping in these two regions, respectively.

We have shown in Sect. 3.2 that PC develops larger changes of the SH tropospheric jet during SON relative to IC. Hence, PC causes surface wind stress and wind stress
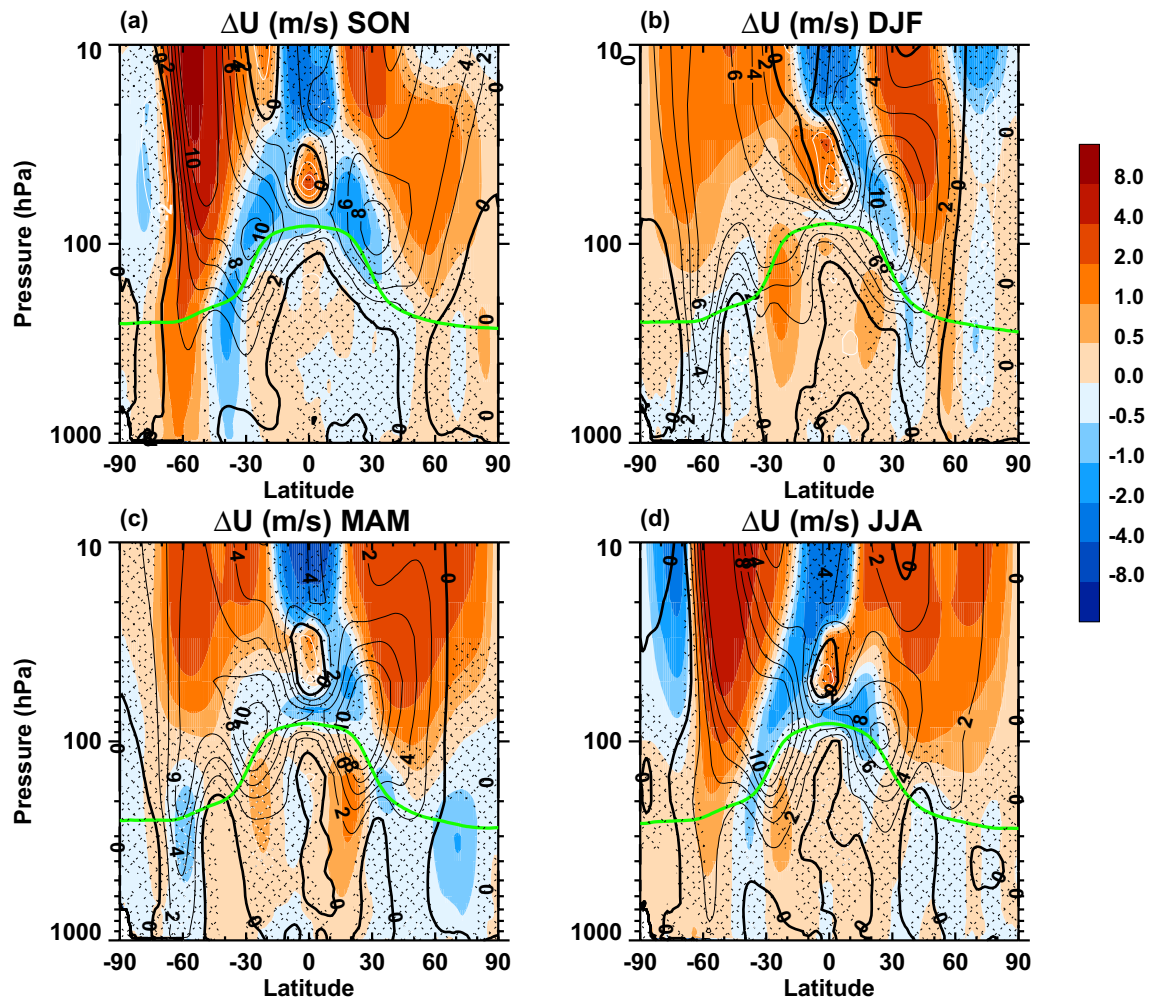
Fig. 8 Different response in the zonal-mean zonal wind to $4 \times CO_2$ between the PC and IC experiment (PC minus IC): **a** September–October–November (SON); **b** December–January–February (DJF); (**c**) March–April–May (MAM); and (**d**) June–July–August (JJA). Contours are the zonal-mean zonal wind response to $4 \times CO_2$ in the IC experiment. Green line is the seasonal mean tropopause level in the IC experiment. Stippling indicates that the difference is not statistically significant at the two-tailed 5% level

Fig. 9 **a** Sea level pressure response to $4 \times CO_2$ in September–October–November (SON) in the IC experiment. **b** Different response to $4 \times CO_2$ between the PC and IC experiment (PC minus IC) in SON sea level pressure. Stippling indicates that the response is not statistically significant at the two-tailed 5% level
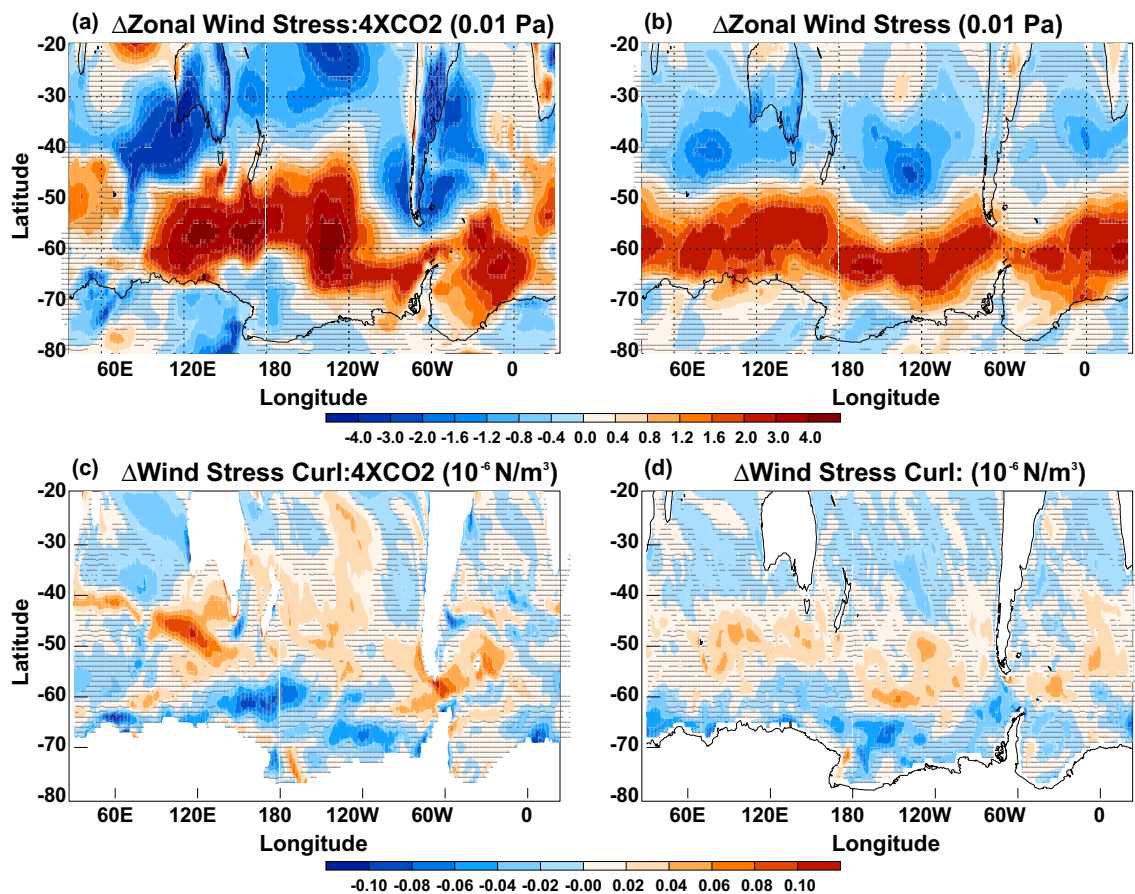
Fig. 10 a Surface zonal wind stress response to $4\times CO_2$ in the IC experiment in September–October–November (SON). **b** Different response in the SON surface zonal wind stress to $4\times CO_2$ between the PC and IC experiment (PC minus IC). Stippling indicates that the response is not statistically significant at the two-tailed 5% level. **c** Same as (**a**), but for wind stress curl. **d** Same as (**b**), but for wind stress curl

curl changes that are too strong during SON relative to IC. Figure 10b shows that neglecting stratospheric chemistry leads to surface westerly wind stress decrease/increase at approximately 45–65°S/30–45°S, respectively. Consequently, the PC simulation induces negative wind stress curl anomalies (Ekman upwelling) south of ~60°S and positive wind stress curl anomalies (Ekman pumping) at ~40–60° S (Fig. 10d). This PC impact is clearly seen in the zonal-mean changes (Fig. 11), which shows a near doubling of wind stress and wind stress curl changes with respect to the IC.

The impact of stratospheric chemistry on the Southern Ocean extends to the deep ocean. The Eulerian MOC streamfunction in the Southern Ocean increases in response to $4\times CO_2$ in IC (Fig. 12a). Prescribed chemistry overestimates the MOC increase poleward of ~50°S and underestimates the MOC increase at ~30–50°S (Fig. 12b), consistent with the surface wind stress changes (Fig. 11a). This is expected because the Eulerian MOC is mostly driven by surface wind stress. The response of the parameterized eddy MOC to stratospheric chemistry is generally opposite to but

is much weaker than the response of the Eulerian MOC (not shown). Hence the net MOC response to stratospheric chemistry is dominated by the Eulerian MOC response.

The stratospheric chemistry impact on the Southern Ocean response to $4\times CO_2$ is strongly seasonal dependent. Only in SON does the PC simulation significantly overestimate changes in surface wind stress, Ekman transport, and MOC, consistent with the seasonality of prescribed chemistry–induced changes in the SH midlatitude tropospheric jet.

3.4 Comparison to stratospheric ozone recovery

The Antarctic ozone hole is projected to recover to its 1980 level around 2070 with the ODS phaseout. Models find that stratospheric ozone recovery plays a crucial role in the twenty-first century SH climate change, mitigating or even canceling SH summertime tropospheric circulation trends caused by increasing GHGs (e.g., Son et al. 2008; Barnes et al. 2014; Previdi and Polvani 2014).
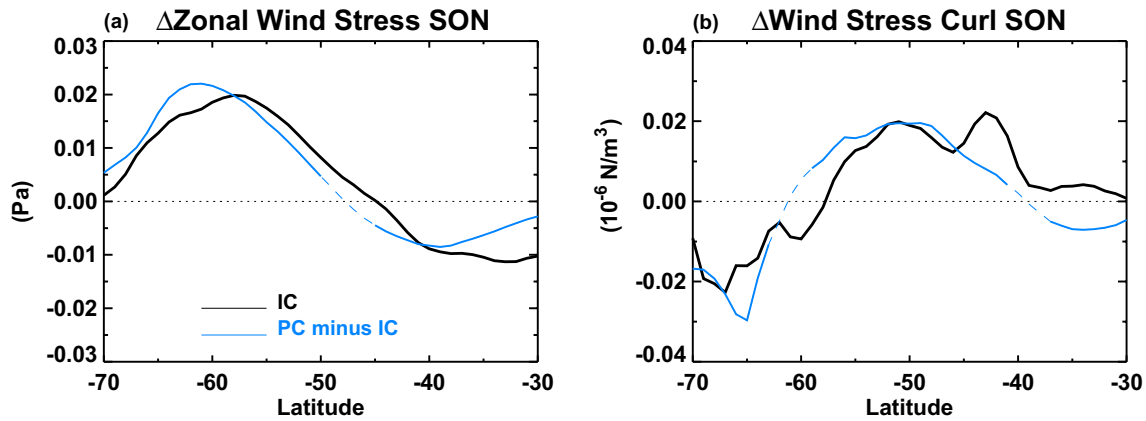
Fig. 11 a Response of the September–October–November zonal-mean surface zonal wind stress to $4 \times CO_2$ in the IC experiment (black line) and the difference response between PC and IC (PC minus IC, blue line). The dashed blue line means the difference is not statistically significant at the two-tailed 5% level. **b** same as (**a**), but for the surface wind stress curl
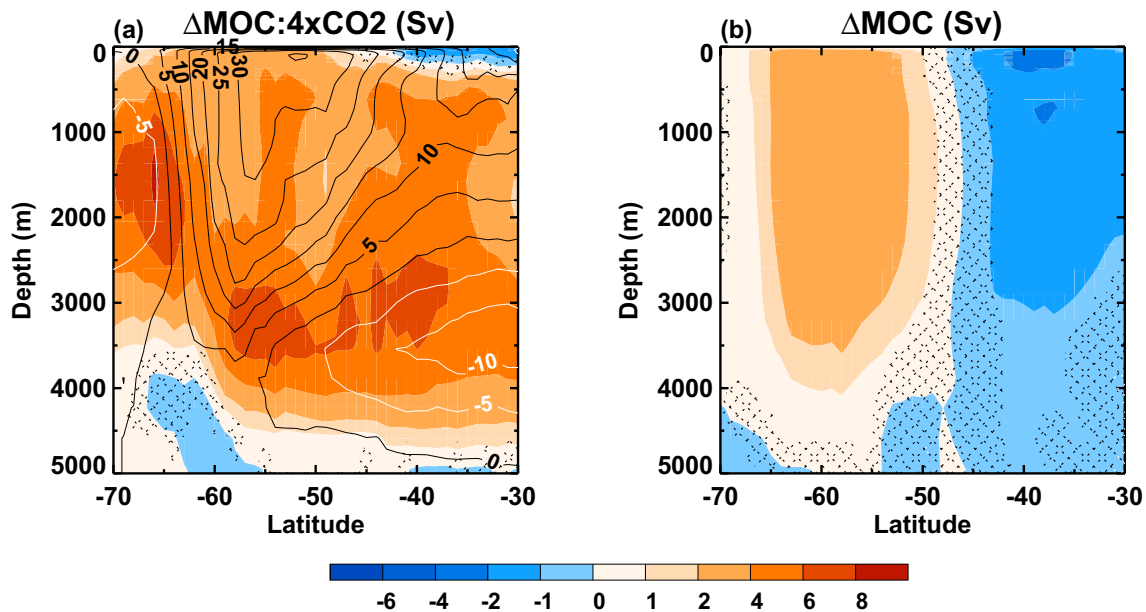

Fig. 12 a Color shading is the Eulerian Meridional Overturn Circulation (MOC) streamfunction response to $4 \times CO_2$ during September–October–November (SON) in the IC experiment. Contours are the climatological field in the IC baseline simulation. **b** Different response in SON MOC streamfunction between PC and IC (PC minus IC). Stippling indicates that the response is not statistically significant at the two-tailed 5% level

Although stratospheric ozone recovery due to decreased ODSs and stratospheric ozone response to $4 \times CO_2$ have similar effects on SH tropospheric circulation, the seasonality of their climate impacts is different. Stratospheric ozone recovery has the largest tropospheric impact in DJF. Stratospheric ozone response to $4 \times CO_2$ in our model, on the other hand, strongly affects SH circulation in SON, but not in DJF. This section aims to better understand the different seasonality from these two stratospheric ozone forcing scenarios.

The stratospheric ozone response to fixed high ODS levels is captured by ozone differences in 2080–2099 between the HighODS and Control simulations. Figure 13 shows that the HighODS simulation yields much lower ozone nearly everywhere in the stratosphere for all seasons. There are some similarities between stratospheric ozone response to high ODSs and stratospheric ozone changes without interaction to $4 \times CO_2$, e.g., largest Antarctic lower stratospheric ozone decrease occurs in SON. There are also significant differences. One major difference is that high ODSs do not
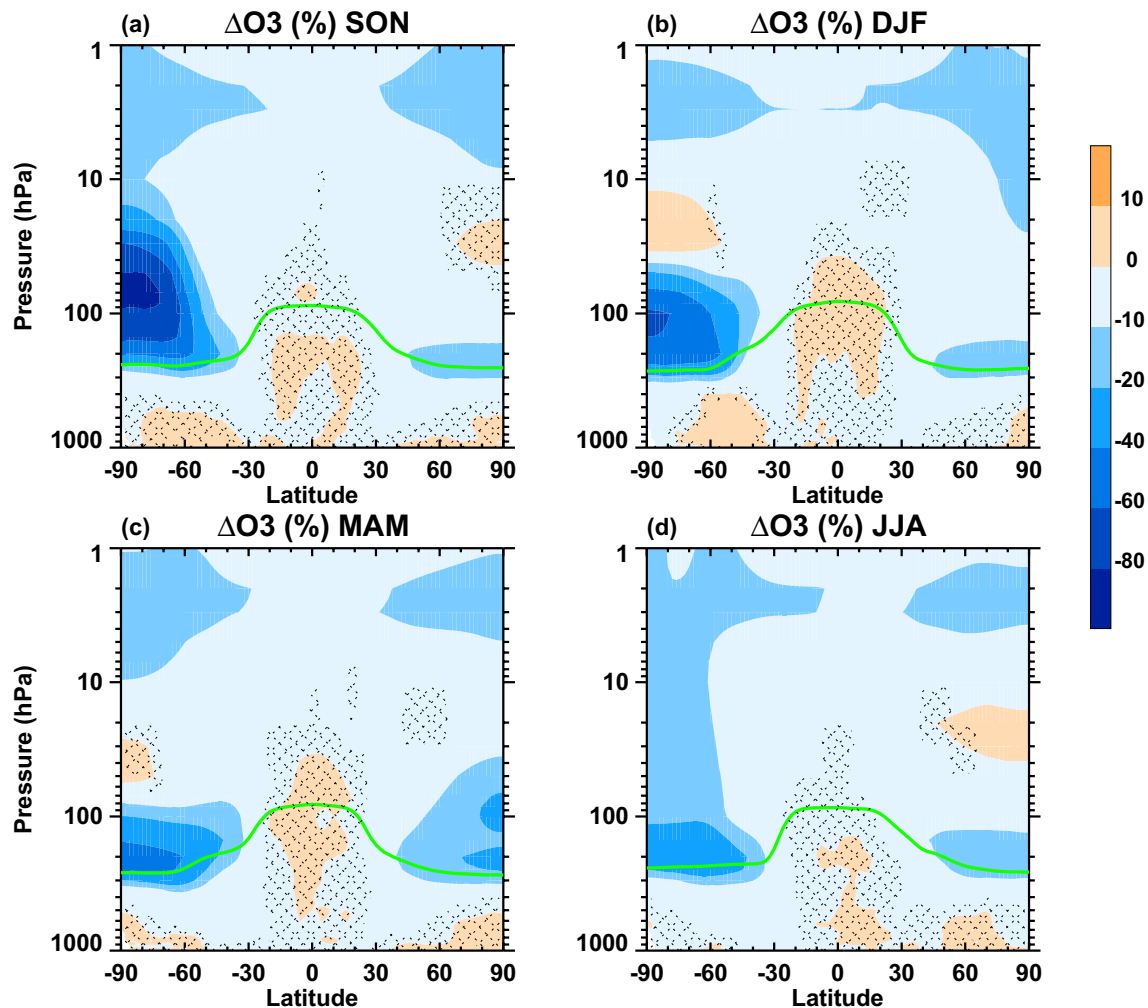
Fig. 13 Seasonal zonal-mean ozone changes in 2080–2099 due to fixing ozone depleting substances at year 2005 levels in (**a**) September–October–November (SON); **b** December–January–February (DJF); **c** March–April–May (MAM); and **d** June–July–August (JJA). Unit is percentage relative to the Control simulation values. Green line is the tropopause level. Stippling indicates that the change is not statistically significant

cause statistically significant tropical lower stratospheric ozone changes. Another major difference is that Antarctic lower stratospheric ozone decreases throughout the year in response to high ODSs, but when interaction with $4 \times CO_2$ is absent Antarctic lower stratospheric ozone increases in DJF (Fig. 6b).

The HighODS simulation includes the effect of increasing GHGs on stratospheric ozone, but the GHG-induced Antarctic ozone change is very small compared to the ODS-induced Antarctic ozone recovery. Fixed high ODSs have the largest impact on Antarctic ozone in SON, with more than 80% lower concentrations between ~ 100 and 40 hPa in the HighODS simulation relative to Control (Fig. 13a). In the absence of Antarctic ozone hole recovery, the Antarctic lower stratosphere is colder from tropopause to 10 hPa in HighODS than in Control (Fig. 14a). The maximum

temperature decrease of more than 8 K is between ~ 90 and 40 hPa, coincident with the maximum ozone decrease. This leads to a stronger meridional temperature gradient that maximizes at around 60°S and 100–40 hPa. The HighODS ozone results in a stronger spring polar vortex jet, with westerly changes in the lower stratosphere centered around 60°S (Fig. 14c). However, statistically significant westerly changes do not reach the tropopause in SON.

High ODSs cause the Antarctic lower stratospheric ozone decrease during DJF. The altitude of the maximum Antarctic ozone decrease descends from 100–40 in SON to 200–80 hPa in DJF (Fig. 13b). The altitude of maximum Antarctic cooling in DJF also descends to around 100 hPa (Fig. 14b), leading to enhanced meridional temperature gradient in the tropopause region. Associated with the descending of the enhanced meridional temperature gradient,
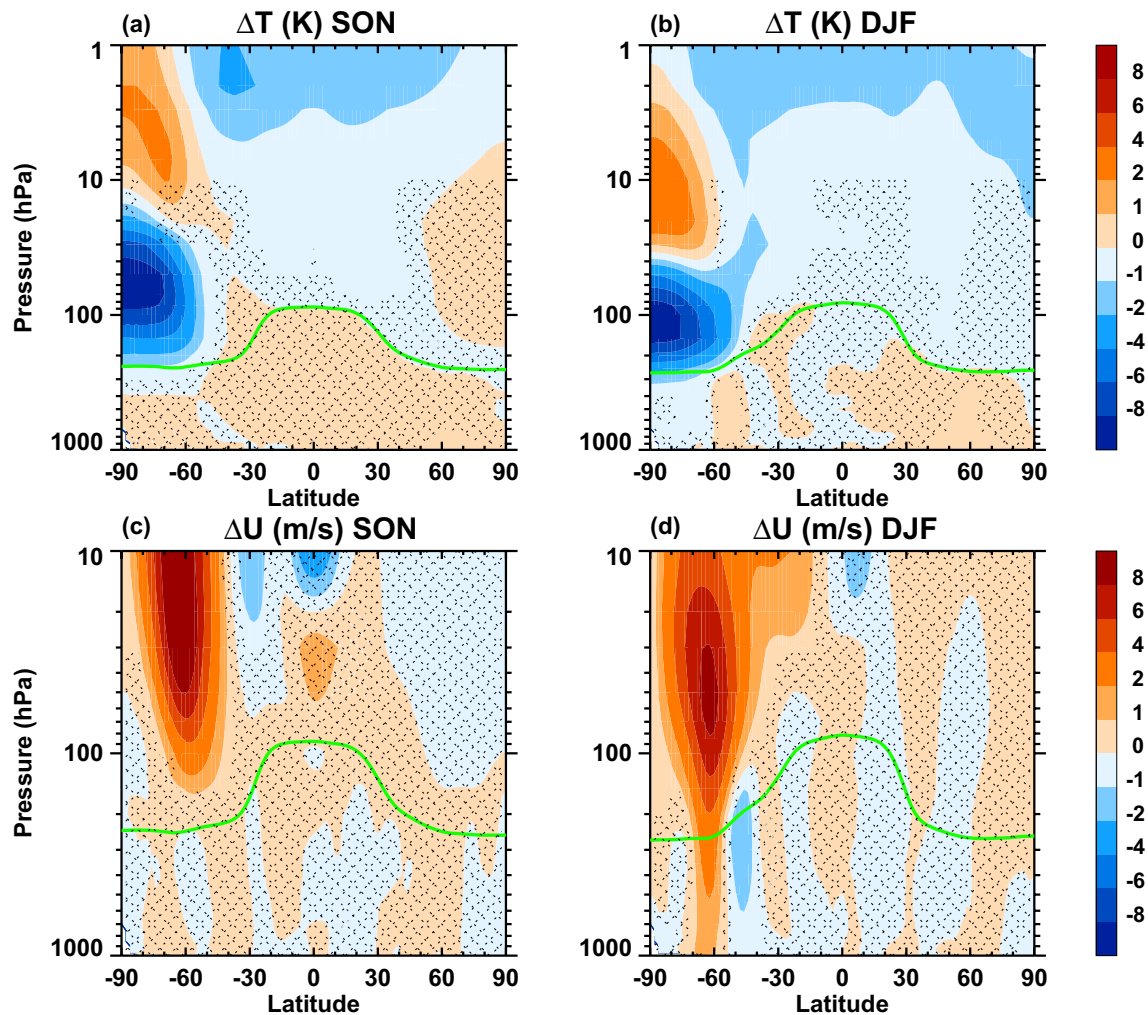
Fig. 14 Zonal-mean temperature changes in 2080–2099 due to fixing ozone depleting substances at year 2005 levels in (**a**) September–October–November (SON); **b** December–January–February (DJF); **c** and **d**: same as (**a**) and (**b**), but for zonal-mean zonal wind. Green line is the tropopause level. Stippling indicates that the change is not statistically significant

statistically significant stratospheric westerly changes descend into troposphere and surface (Fig. 14d).
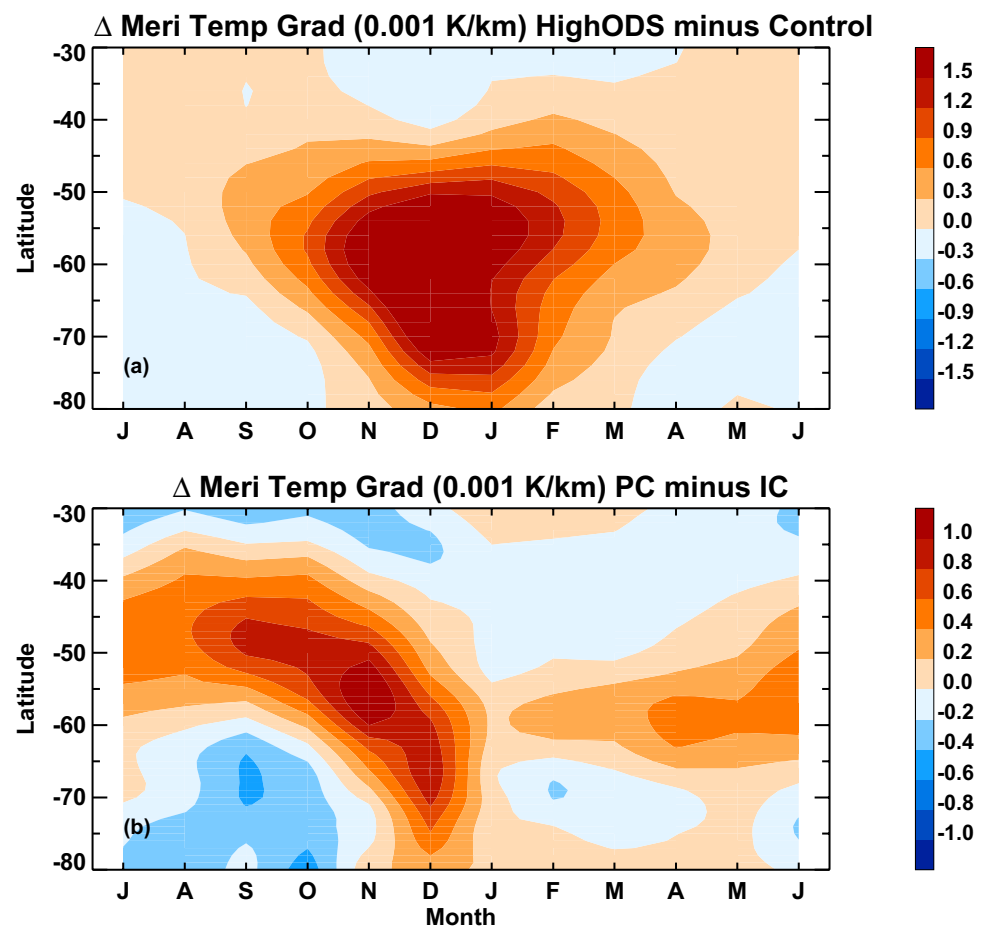
The above analyses suggest that the seasonality of meridional temperature gradient change in the tropopause region is important to determine the seasonality of the downward coupling of stratospheric circulation anomalies. Figure 15a shows the seasonal evolution of meridional temperature gradient change in the SH extratropical tropopause region (averaged between 250 and 150 hPa) caused by high ODSs. Consistent with the analyses above, the largest increase of meridional temperature gradient near the tropopause does not occur in SON, but in DJF. In the case of neglecting Antarctic ozone response to $4 \times CO_2$, however, the seasonality of tropopause temperature gradient change is quite different (Fig. 15b). The strongest meridional temperature gradient increase is found in SON, and the weakest temperature gradient increase is in January and February (Fig. 15b).

Therefore, the different seasonality of SH tropospheric jet impact in these two stratospheric ozone change scenarios could be explained by the different seasonality of tropopause meridional temperature gradient change.

4 Conclusions

The response of the stratospheric ozone layer to quadrupled CO_2 concentrations and its climate impact are investigated. Two abrupt $4 \times CO_2$ experiments with interactive and prescribed stratospheric chemistry were conducted, respectively, using the coupled atmosphere–ocean GEOSCCM. The effects of interactive stratospheric chemistry on stratospheric and tropospheric temperature and circulation, including their seasonal variations, are quantified by comparing these two experiments.

Fig. 15 Seasonal evolution of meridional temperature gradient change in the Southern Hemisphere extratropical tropopause region (averaged over 250–150 hPa) (**a**) due to fixing ozone depleting substances at years 2005 levels (HighODS minus Control); (**b**) due to neglecting stratospheric ozone response to $4\times CO_2$ (PC minus IC)

The global mean surface temperature response to $4\times CO_2$ in the interactive and prescribed chemistry experiments is similar, i.e., the stratospheric chemical feedback is small in GEOSCCM. Interactive chemistry only modifies the climate feedback parameter in GEOSCCM by -0.02 W m^{-2} K^{-1}, resulting in a 0.16 K (2.4%) reduction of global-mean surface warming in response to $4\times CO_2$. This result is consistent with Marsh et al. (2016) and Chiodo et al. (2019) that including interactive stratospheric ozone chemistry is not important in determining the climate sensitivity.

Nevertheless, stratospheric chemistry is necessary to capture the SH tropospheric midlatitude jet response to $4\times CO_2$. Neglecting interactive stratospheric ozone in a $4\times CO_2$ simulation leads to a warmer tropical lower stratosphere and a cooler polar lower stratosphere. The resulting stronger negative equator-to-pole meridional temperature gradient results in excessive strengthening of the midlatitude stratospheric westerlies. In the SH, this impact extends to the troposphere, yielding a stronger poleward shift and intensification of the tropospheric midlatitude jet than occurs with interactive stratospheric chemistry.

A focus of this paper is to understand the seasonal variations of the stratospheric chemistry-induced climate impact.

We find that stratospheric chemistry has significant effects on the SH tropospheric and Southern Ocean circulation only in the austral spring season SON. The seasonal evolution of the Antarctic polar vortex and the Brewer-Dobson circulation leads to large Antarctic lower stratospheric ozone increase during SON in response to $4\times CO_2$. Without interactive chemistry, the reduced ozone shortwave absorption, together with the associated dynamical cooing, causes much colder Antarctic lower stratosphere and much stronger stratospheric westerly response during SON. Associated with the stratospheric circulation changes, the prescribed chemistry experiment significantly overestimates SH tropospheric midlatitude jet response to $4\times CO_2$, amplifying its poleward shift by 250% and the strengthening of the jet maximum by 62% during SON compared to the interactive chemistry experiment. It should be noted that, though, the annual mean SH tropospheric midlatitude jet response is much weaker than that in SON. Prescribed chemistry also underestimates the interannual variability of the Antarctic polar vortex in the austral spring and early summer.

Neglecting stratospheric chemical interaction overestimates climate response to $4\times CO_2$ on the SH surface and the Southern Ocean during SON. The prescribed chemistry

experiment produces stronger surface wind stress responses that doubles those in the interactive chemistry experiment. Consequently, prescribed chemistry substantially overestimates responses of Ekman pumping/upwelling and meridional overturning circulation in the Southern Ocean during SON.

The seasonality of interactive chemistry-induced tropospheric dynamical effect is different between this study and Chiodo and Polvani (2017, 2019), who have showed that stratospheric ozone response to $4 \times CO_2$ has largest impact on tropospheric circulation in DJF. This difference can be attributed to the different experimental setup, particularly the ODS levels in the baseline simulation. Our experiment is based on 2000 conditions, which has much higher ODS loading the previous studies that are based on preindustrial conditions. In our interactive chemistry $4 \times CO_2$ experiment, the Antarctic heterogeneous ozone destruction is enhanced due to CO_2-induced cooling and high ODS levels. This chemistry ozone loss competes with dynamics-driven Antarctic ozone increase, leading to ozone decrease in the summer Antarctic lower stratosphere. As a result, the meridional temperature gradient increase in the SH tropopause region is much weaker in DJF than in SON, which explains why interactive chemistry significantly affect tropospheric and ocean circulation in SON but not in DJF in our experiment.

Stratospheric ozone recovery significant affects SH climate change in the twenty-first century. However, the seasonality of the climate impact of ODS-caused stratospheric ozone recovery and $4 \times CO_2$-caused stratospheric ozone changes is different. Notably, interactive and prescribed chemistry produce similar effects on the SH tropospheric circulation in DJF, when stratospheric ozone recovery has the largest climate impact. This different seasonality is related to the different seasonality of Antarctic lower stratospheric ozone response and the tropopause meridional temperature gradient change in these two scenarios.

Stratospheric chemical feedback on global-mean surface temperature is an important metric to quantify the climate impact of stratospheric chemistry under $4 \times CO_2$ forcing. However, it does not capture the effects of stratospheric chemistry on tropospheric and oceanic circulations. Despite differences in models and experimental setup, results from this study and Chiodo and Polvani (2017, 2019) show that including stratospheric ozone response to increased CO_2 is essential to simulate the SH dynamical sensitivity and its seasonal variability.

Studies of interactive stratospheric chemistry impact on troposphere and surface, including this study, focus on long-term climate timescale. However, the stratosphere-troposphere dynamical coupling mechanisms, although not fully understood, appear to operate across different timescales [Kidston et al. 2015]. At the subseasonal-to-seasonal (S2S) timescale, stratospheric variability, such as the stratospheric sudden warmings events, is an important source of surface predictability [Baldwin et al. 2003; Domeisen et al. 2020]. Note that interactive stratospheric ozone chemistry is not implemented in current S2S prediction systems. Whether interactive stratospheric ozone could provide a potential source to enhance surface S2S forecast skills may be a key area for stratosphere-troposphere coupling.

Declarations

Conflict of interest The authors declare no conflicts of interest.

References

Andrews T, Gregory JM, Webb MJ (2015) The dependence of radiative forcing and feedback on evolving patterns of surface temperature change in climate models. J Clim 28:1630–1648. https://doi.org/10.1175/JCLI-D-14-00545.1

Baldwin D, Stephenson B, Thompson DWJ, Dunkerton TJ, Charlton AJ, O'Neill A (2003) Stratospheric memory and skill of extended-range weather forecasts. Science 301:636–640. https://doi.org/10.1126/science.1087143

Banerjee A, Chiodo G, Previdi M, Ponater P, Conley AJ, Polvani LM (2019) Stratospheric water vapor: an important climate feedback. Clim Dyn 53:1697–1710. https://doi.org/10.1007/s00382-019-04721-4

Barnes EA, Barnes NW, Polvani LM (2014) Delayed Southern Hemisphere climate change induced by stratospheric ozone recovery, as projected by the CMIP5 models. J Clim 27:852–867. https://doi.org/10.1175/JCLI-D-13-00246.1

Butchart N, Scaife AA, Bourqui M, de Grandpr'e J, Hare SHE, Kettleborough J, Langematz U, Manzini E, Sassi F, Shibata K, Shindell D, Sigmond M (2006) Simulations of anthropogenic change in the strength of the Brewer-Dobson circulation. Clim Dyn 27:727–741. https://doi.org/10.1007/s00382-006-0162-4

Butchart N et al (2010) Chemistry-climate model simulations of 21st century stratospheric climate and circulation changes. J Clim 23:5349–5374. https://doi.org/10.1175/2010JCLI3404.1

Chiodo G, Polvani LM (2017) Reduced Southern Hemispheric circulation response to quadrupled CO$_2$ due to stratospheric ozone feedback. Geophys Res Lett 44:465–474. https://doi.org/10.1002/2016GL071011

Chiodo G, Polvani LM, Marsh D, Stenke A, Ball W, Rozanov E, Muthers S, Tsigaridis K (2018) The response of the ozone layer to quadrupled CO$_2$ concentrations. J Clim 31:3893–3907. https://doi.org/10.1175/JCLI-D-17-0492.1

Chiodo G, Polvani LM (2019) The response of the ozone layer to quadrupled CO$_2$ concentrations: Implication for climate. J Clim 32:7629–7642. https://doi.org/10.1175/JCLI-D-19-0086.1

Dessler A, Schoeberl M, Wang T, Davis S, Rosenlof K (2013) Stratospheric water vapor feedback. Proc Natl Acad Sci USA 110(45):18087–18091. https://doi.org/10.1073/pnas.1310344110

Dietmüller S, Ponater M, Sausen R (2014) Interactive ozone induces a negative feedback in CO2-driven climate change simulations. J Geophys Res Atmos 119:1796–1805. https://doi.org/10.1002/2013JD020575

Domeisen DIV, Butler AH, Charlton-Perez AJ, Ayarzagüena B, Baldwin MP, Dunn-Sigouin E et al. (2020) The role of the stratosphere in subseasonal to seasonal prediction: 2. Predictability arising from stratosphere-troposphere coupling. J Geophys Res Atmos 125:e2019JD030923. https://doi.org/10.1029/2019JD030923

Gregory JM (2004) A new method for diagnosing radiative forcing and climate sensitivity. Geophys Res Lett 31:L03205. https://doi.org/10.1029/2003GL018747

Griffies SM (2012) Elements of the modular ocean model (MOM) (2012 Release). In: GFDL Ocean Group Technical Report No. 7

Hunke EC, Lipscomb WH (2008) CICE: the Los Alamos Sea ice model documentation and software manual (version 4.0). Tech. Rep, Los Alamos National Laboratory, p 116

Jonsson AI, De Grandpre J, Fomichev VI, McConnell JC, Beagley SR (2004) Doubled CO2-induced cooling in the middle atmosphere: photochemical analysis of the ozone radiative feedback. J Geophys Res 109:D24103. https://doi.org/10.1029/2004JD005093

Kidston J, Scaife AA, Hardiman SC, Mitchell DM, Butchart N, Baldwin MP, Gray LJ (2015) Stratospheric influence on tropospheric jet streams, storm tracks and surface weather. Nat Geosci 8:433–440. https://doi.org/10.1038/NGEO2424

Kushner PJ, Held IM, Delworth TL (2001) Southern Hemisphere atmospheric circulation response to global warming. J Clim 14:2238–2249

Li F, Newman PA (2020) Stratospheric water vapor feedback and its climate impacts in the coupled atmosphere-ocean Goddard Earth Observing System Chemistry-Climate Model. Clim Dyn 55(5):1585–1595. https://doi.org/10.1007/s00382-020-05348-6

Li F, Austin J, Wilson J (2008) The strength of the Brewer—Dobson circulation in a changing climate: coupled chemistry climate model simulations. J Clim 21:40–57. https://doi.org/10.1175/2007JCLI1663.1

Li F, Stolarski RS, Newman PA (2009) Stratospheric ozone in the post-CFC era. Atmos Chem Phys 9:2207–2213

Li F, Vikhliaev YV, Newman PA, Pawson S, Perlwitz J, Waugh DW, Douglass AR (2016) Impacts of interactive stratospheric chemistry on Antarctic and Southern Ocean climate change in the Goddard Earth Observing System, Version 5 (GEOS-5). J Clim 29:3199–3218. https://doi.org/10.1175/JCLI-D-15-0572.1

Lin P, Paynter D, Polvani L, Correa GJP, Ming Y, Ramaswamy V (2017) Dependence of model-simulated response to ozone depletion on stratospheric polar vortex climatology. Geophys Res Lett. https://doi.org/10.1002/2017GL073862

Lu J, Chen G, Frierson DMW (2008) Response of the zonal mean atmospheric circulation to El Nino versus global warming. J Clim 21:5835–5851. https://doi.org/10.1175/2008JCLI2200.1

Marsh DR, Lamarque J-F, Conley AJ, Polvani LM (2016) Stratospheric ozone chemistry feedbacks are not critical for the determination of climate sensitivity in CESM1(WACCM). Geophys Res Lett 43:3928–3934. https://doi.org/10.1002/2016GL068344

Marshall J, Speer K (2012) Closure of the meridional overturning circulation through Southern Ocean upwelling. Nat Geosci 5(3):171–180. https://doi.org/10.1038/ngeo1391

Molod A, Takacs L, Suare, M, Bacmeister J, Song IS, Eichmann A (2012) The GEOS-5 atmospheric general circulation model: Mean climate and development from MERRA to Fortuna. Technical Report Series on Global Modeling and Data Assimilation, Rep. 28, 115 pp, Available online at http://gmao.gsfc.nasa.gov/pubs/docs/Molod484.pdf.]

Nowack PJ, Abraham NL, Maycock AC, Braesicke P, Gregory JM, Joshi MM, Osprey A, Pyle JA (2015) A large ozone-circulation feedback and its implications for global warming assessments. Nat Clim Change 5:41–45. https://doi.org/10.1038/nclimate2451

Oman LD, Douglass AR (2014) Improvements in total column ozone in GEOSCCM and comparisons with a new ozone-depleting substances scenario. J Geophys Res Atmos 119:5613–5624. https://doi.org/10.1002/2014JD021590

Pawson S, Stolarski RS, Douglass AR, Newman PA, Nielsen JE, Frith SM, Gupta ML (2008) Goddard earth observing system chemistry–climate model simulations of stratosphere ozone–temperature coupling between 1950 and 2005. J Geophys Res 113:D12103. https://doi.org/10.1029/2007JD009511

Previdi M, Polvani LM (2014) Climate system response to stratospheric ozone depletion and recovery. Q J R Meteorol Soc. https://doi.org/10.1002/qj.2330

Russell JL, Dixon KW, Gnanadesikan A, Stouffer J, Toggweiler JR (2006) The southern hemisphere westerlies in a warming world: propping open the door to the deep ocean. J Clim 19:6382–6390

Shepherd TG (2008) Dynamics, stratospheric ozone, and climate change. Atmos Ocean 46:117–138. https://doi.org/10.3137/ao.460106

Son S-W, Polvani LM, Waugh DW, Akiyoshi H, Garcia R, Kinnison D, Pawson S, Rozanov E, Shepherd TG, Shibata K (2008) The impact of stratospheric ozone recovery on the Southern Hemisphere westerly jet. Science 320:1486–1489. https://doi.org/10.1126/science.1155939